

Spin States and Stability of Fe^{III} Complexes of Ligands with Carboxamido Nitrogen and Phenolato Oxygen Donors

Dana S. Marlin,^[a] Marilyn M. Olmstead,^[b] and Pradip K. Mascharak*^[a]

Keywords: Iron / N ligands / O ligands / Spin states

As part of our attempts to prepare Fe^{III} complexes with “tunable” spin states, we have synthesized three novel six-coordinate Fe^{III} complexes containing both carboxamido nitrogen (N_{amido}) and phenolato oxygen (O_{phen}) donors in their ligand framework. Since it has already been shown that carboxamido nitrogen donors usually stabilize Fe^{III} in a low spin configuration, while phenolato oxygens tend to stabilize Fe^{III} in a high spin state, we have incorporated both donor groups in our designed ligands. The syntheses and structures of Fe^{III}

complexes with either one or two N_{amido} and O_{phen} donors are reported in this paper. The properties of these complexes have been compared with the properties of analogous Fe^{III} complexes. The competing effects of N_{amido} and O_{phen} on the spin state of the Fe^{III} center are discussed in terms of the stabilities of the overall complexes.

(© Wiley-VCH Verlag GmbH, 69451 Weinheim, Germany, 2002)

Introduction

Monomeric complexes with stable Fe^{III} centers are attractive synthetic targets to inorganic chemists for their use, among other things, as catalysts, enzyme mimics, or as model complexes that allow for detailed study of the electronic properties of the Fe^{III} center.^[1–4] Recent work from this laboratory in conjunction with the work of others has shown that coordination of a carboxamido nitrogen (N_{amido}) to an Fe^{III} center makes it resistant toward hydrolytic decomposition.^[5] Furthermore, the reduction potential of the Fe^{III} center is shifted toward more negative values by approximately –0.5 V per N_{amido} to a maximum of about –1.10 V.^[5,6] In addition, the majority of the six-coordinate Fe^{III} complexes with one, two, and four N_{amido} donors possess low spin (LS) ground states.^[3,5,6] Wieghardt and co-workers have performed extensive studies to evaluate the electronic and physical properties of mononuclear Fe^{III} complexes with Fe^{III}–O_{phen} (O_{phen} = phenolato O) bonds.^[7–8] They have pointed out that the majority of these complexes tend to have high spin (HS) Fe^{III} centers (with a t_{2g}³e_g² electronic configuration) and that Fe^{III}–O_{phen} bonds are often short, indicating considerable double bond character with ligand-to-metal d_π–p_π back bonding.^[9] We decided to combine both Fe^{III}–N_{amido} and Fe^{III}–O_{phen} interactions within the same Fe^{III} complex with the intention of

obtaining Fe^{III} complexes with “tunable” spin states. In the long term, we intend to gain control over (a) the redox potential, (b) stability and (c) the spin state of the Fe^{III} center, all of which influence its reactivity. Here we report the results of our initial effort toward this goal.

Previously, we have described the structure and chemistry of Fe^{III} complexes of the pentadentate ligand *N,N'*-bis(2-hydroxyphenyl)-pyridine-2,6-dicarboxamide (POPYH₄) (Figure 1).^[10] When deprotonated, this ligand becomes planar and coordinates to the Fe^{III} center in the basal plane of a pentagonal bipyramid. The HS Fe^{III} complexes of this ligand namely, [Fe(POPY)(L)₂]^{n–} (L = SCN[–], *N*-methylimidazole), were the first examples of structurally characterized species in which both N_{amido} and O_{phen} donors are coordinated to the Fe^{III} center in the same complex. We have now prepared additional six-coordinate complexes with similar ligands in order to explore the properties of these types of complexes in more detail. The two designed ligands that have been employed in this study are the tridentate ligand *N*-(2-hydroxyphenyl)-2-pyridinecarboxamide (PypepOH₂) and the pentadentate ligand *N,N*-bis(2-pyridylmethyl)amine-*N*-ethyl-2-hydroxyphenyl-2-carboxamide (Papy₂OH₂) (Figure 1). In both PypepOH₂ and Papy₂OH₂, the H's represent dissociable phenolic and carboxamide hydrogens. In the deprotonated forms, these ligands coordinate to Fe^{III} to afford stable HS six-coordinate complexes Na[Fe(PypepO)₂] (**1**), and [Fe(Papy₂O)(L)] (**2** L = Cl[–]; **3** L = SCN[–]). These complexes represent only the second and third set of examples of structurally characterized complexes with Fe^{III} centers coordinated to both N_{amido} and O_{phen} donors. They are also the first such examples of six-coordinate Fe^{III} complexes. The structural and spectro-

^[a] Department of Chemistry and Biochemistry, University of California, Santa Cruz, Santa Cruz, CA 95064, USA
Fax: (internat.) + 1-831/459-2935
E-mail: pradip@chemistry.ucsc.edu

^[b] Department of Chemistry, University of California, Davis, Davis, CA 95616, USA

scopic properties of these complexes (with both $\text{Fe}^{\text{III}}-\text{N}_{\text{amido}}$ and $\text{Fe}^{\text{III}}-\text{O}_{\text{phen}}$ bonds) have been compared with Fe^{III} complexes with either $\text{Fe}^{\text{III}}-\text{O}_{\text{phen}}$ or $\text{Fe}^{\text{III}}-\text{N}_{\text{amido}}$ bonds.

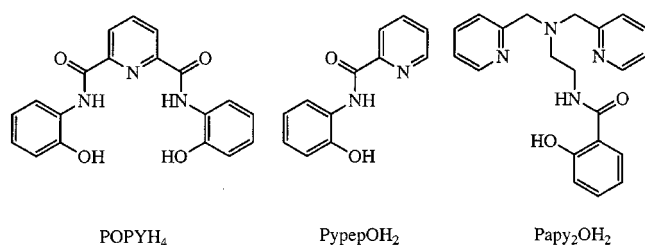


Figure 1. Ligands that contain both N_{amido} and O_{phen} donors used in previous (POPYH_4) and the present study (PypepOH_2 and Papy_2OH_2); the H's in POPYH_4 , PypepOH_2 and Papy_2OH_2 represent dissociable phenolate and carboxamide hydrogens

Results and Discussion

The tridentate ligand PypepOH_2 was prepared by reacting 2-aminophenol with 2-pyridinecarbonyl chloride (the latter prepared from 2-picolinic acid and thionyl chloride) in tetrahydrofuran (THF). The acetate-protected derivative of the pentadentate ligand Papy_2OH_2 , namely $\text{Papy}_2\text{OC}-\text{OCH}_3$, was synthesized from (2-aminoethyl)bis(2-pyridylmethyl)amine and 2-acetylphenylcarbonyl chloride (the latter prepared from 2-acetylsalicylic acid and oxalyl chloride). Pure Papy_2OH_2 was obtained in good yield following deprotection of $\text{Papy}_2\text{OCOCH}_3$ with NaOH and neutralization with HCl. For ease of handling, Papy_2OH_2 was converted into the mono-sodium salt NaPapy_2OH by reaction of Papy_2OH_2 with NaOMe in MeOH. Reaction of $[\text{Fe}(\text{DMF})_6](\text{ClO}_4)_3$ with two equiv. of PypepOH_2 and four equiv. of NaH (both relative to iron) in DMF afforded the Fe^{III} complex $\text{Na}[\text{Fe}(\text{PypepO})_2]$ (**1**). The dark red complex $[\text{Fe}(\text{Papy}_2\text{O})(\text{Cl})]$ (**2**) was synthesized by reacting $(\text{Et}_4\text{N})[\text{FeCl}_4]$ with NaPapy_2OH plus one equiv. of NaH in DMF. Reaction of $[\text{Fe}(\text{DMF})_6](\text{ClO}_4)_3$ with one equiv. of $\text{Papy}_2\text{O}^{2-}$ in DMF followed by one equiv. of NaSCN resulted in the formation of $[\text{Fe}(\text{Papy}_2\text{O})(\text{NCS})]$ (**3**) in high yield.

Molecular Structure of $\text{Na}[\text{Fe}(\text{PypepO})_2]$ (**1**)

X-ray quality crystals of $\mathbf{1} \cdot 2.5\text{CH}_3\text{CN}$ were grown from a saturated solution of **1** in CH_3CN , upon cooling to -20°C . The structure of the complex shows two deprotonated PypepO^{2-} ligands coordinated to an Fe^{III} center in a *mer* geometry (Figure 2a). In the solid state, $\mathbf{1} \cdot 2.5\text{CH}_3\text{CN}$ forms an elaborate network of $[\text{Fe}(\text{Pypep})_2]^-$ and Na^+ ions bridged through carbonyl and phenolato oxygens with additional coordination of CH_3CN to the Na^+ center. The lattice structure is built up of dimeric $[\text{Fe}(\text{PypepO})_2]^- \cdots \text{Na}^+ \cdots [\text{Fe}(\text{PypepO})_2]^- \cdots \text{Na}^+$ units which in turn are connected together into an extended network with large pockets formed by four such dimeric units (Fig-

ure 2b). This arrangement creates small pockets at the center of each dimer and large pockets by the four-dimer clusters. Some of the large pockets are occupied by uncoordinated CH_3CN molecules (Figure 2b).

It is interesting to note that like complex **1**, $\text{Na}[\text{Fe}(\text{POPY})(\text{N-MeIm})_2] \cdot 3\text{CH}_3\text{CN}$ also forms an extended structure in the solid state with Na^+ bonded to phenolate and carbonyl oxygen donors from the POPY^{4-} ligand and lattice CH_3CN molecules.^[10] However, in the case of $\text{Na}[\text{Fe}(\text{POPY})(\text{N-MeIm})_2] \cdot 3\text{CH}_3\text{CN}$, polymeric chains form between monomeric $\text{Na}^+ \cdots [\text{Fe}(\text{POPY})(\text{N-MeIm})_2]^-$ units in the lattice, which differs considerably from the elaborate porous network seen in $\mathbf{1} \cdot 2.5\text{CH}_3\text{CN}$. Also, the bond lengths for **1** $\text{Fe}^{\text{III}}-\text{N}_{\text{amido}}$ [av. 2.064(4) Å] and $\text{Fe}^{\text{III}}-\text{O}_{\text{phen}}$ [av. 1.962(4) Å] as well as $\text{Fe}^{\text{III}}-\text{N}_{\text{py}}$ [av. 2.178(5) Å] (*py* = pyridine) are substantially shorter than analogous bond lengths in $\text{Na}[\text{Fe}(\text{POPY})(\text{N-MeIm})_2]$ (av. 2.228 Å, 2.045 Å, and 2.221 Å respectively) due to the ligand strain imposed by the pentadentate planar POPY^{4-} ligand in the latter complex.

Molecular Structures of $[\text{Fe}(\text{Papy}_2\text{O})(\text{Cl})]$ (**2**) and $[\text{Fe}(\text{Papy}_2\text{O})(\text{SCN})]$ (**3**)

X-ray quality crystals of $\mathbf{2} \cdot 2\text{CH}_3\text{CN}$ were grown from CH_3CN at -20°C while a toluene/ CH_2Cl_2 (3:1) mixture was used to obtain single crystals of **3**·toluene. Both **2** and **3** are monomeric and the coordination geometry is octahedral with the deprotonated $\text{Papy}_2\text{O}^{2-}$ ligand coordinated to five of the six sites of the Fe^{III} center in both complexes. In **2**, a Cl^- ion occupies the sixth site (Figure 3) while in **3**, the sixth site is occupied by a SCN^- ion (Figure 4).

Since these complexes are neutral, there is no extended structure in solid state. The bond lengths of **2** and **3** are similar (Table 1). The $\text{Fe}^{\text{III}}-\text{N}_{\text{amido}}$ [av. 2.0157(14) Å] and $\text{Fe}^{\text{III}}-\text{N}_{\text{py}}$ [av. 2.1511(15) Å] bond lengths of **2** and **3** compare well with those noted for **1** while the $\text{Fe}^{\text{III}}-\text{O}_{\text{phen}}$ distance [av. 1.8781(12) Å] is slightly shorter. The $\text{N}_{\text{amido}}-\text{Fe}-\text{O}_{\text{phen}}$ angles in both **2** and **3** are larger (91° , six-membered rings) than the same angles in **1** (av. 80° , five-membered rings, Table 1).

Stability and Spectroscopic Properties

The EPR spectra of **1**, **2**, and **3** in DMF glass clearly indicate that the Fe^{III} centers in these complexes exist as HS. During the past few years, we have synthesized several similar Fe^{III} complexes that contain one, two or four $\text{Fe}^{\text{III}}-\text{N}_{\text{amido}}$ bonds in addition to $\text{Fe}^{\text{III}}-\text{N}_{\text{py}}$ and/or $\text{Fe}^{\text{III}}-\text{S}_{\text{thio}}$ (thio = thiophenolato) bonds.^[5,11-14] All these complexes are consistently LS (Table 2). The obvious difference between the present set of complexes (**1**, **2**, and **3**) and the rest of the entries in Table 2 is the fact that complexes **1**, **2**, and **3** contain $\text{Fe}^{\text{III}}-\text{O}_{\text{phen}}$ bonds. In general, mononuclear Fe^{III} complexes with either one,^[7,15,16] two,^[17] three^[8,18] or four^[10,19] $\text{Fe}^{\text{III}}-\text{O}_{\text{phen}}$ bonds all tend to possess HS ($t_{2g}^3e_g^2$) Fe^{III} centers. The $\text{Fe}^{\text{III}}-\text{O}_{\text{phen}}$ bond in the majority of these complexes has been described as more than a single bond with additional $d_{\pi}-p_{\pi}$ back-bonding.^[9] Wiegh-

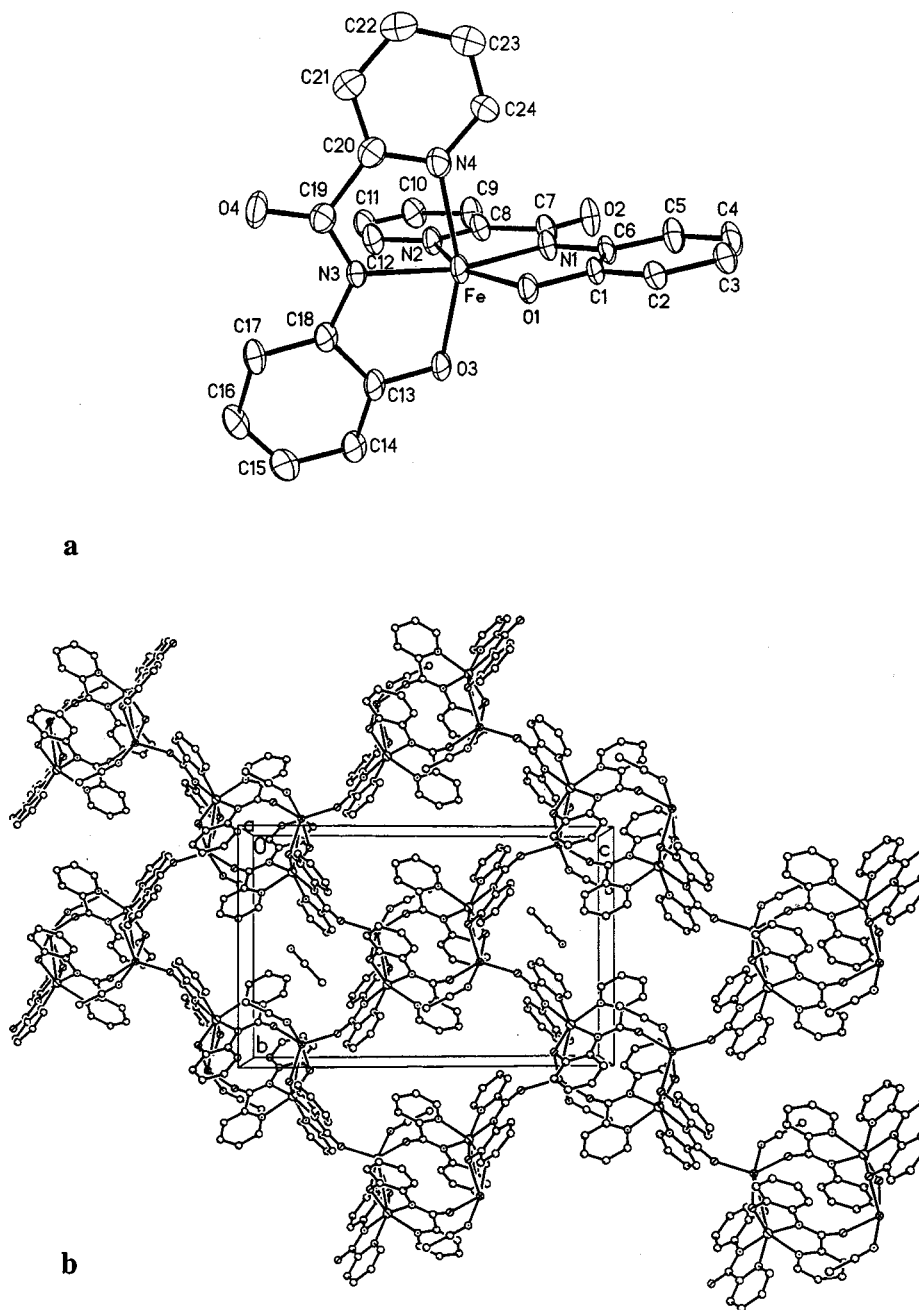
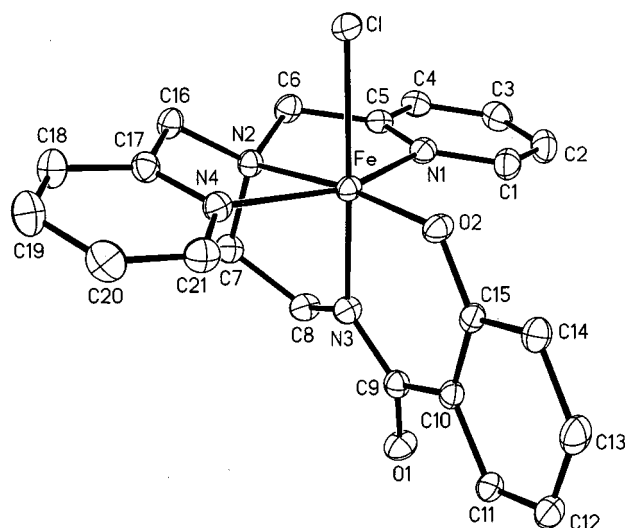
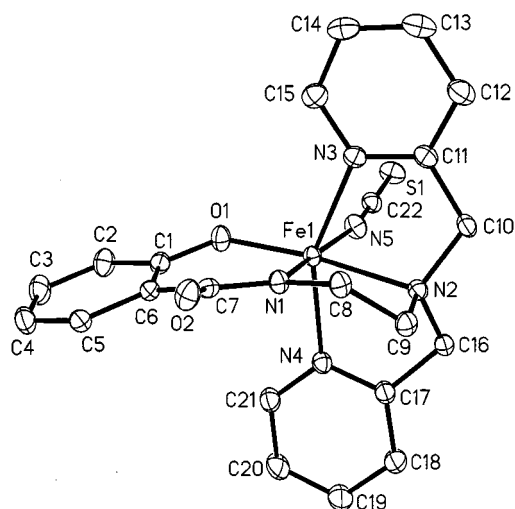


Figure 2. (a) Thermal ellipsoid plot of [Fe(PypepO)₂]⁺ (at the 35% probability level); (b) extended structure of Na[Fe(PypepO)₂]·2.5CH₃CN showing the small and large pockets formed in the solid state

ardt and co-workers have suggested that the HS configuration of the Fe^{III} center facilitates such a d_{π} - p_{π} interaction.^[9] Since the Fe^{III}-O_{phen} distances in complexes **1**, **2**, and **3** (Table 1) compare well with the “short” Fe^{III}-O_{phen} distances reported so far (range = 1.85–1.97 Å),^[7–10,15–19] it is evident that the Fe^{III}-O_{phen} bonds in **1**, **2**, and **3** are of a similar nature, and hence these complexes prefer a HS configuration. Taken together, these facts indicate that when the Fe^{III} center is coordinated to both carboxamido nitrogen(s) and phenolato oxygen(s) (like **1**, **2**, and **3**), the

Fe^{III}-O_{phen} interaction dominates and the resultant complexes are HS.

A change in spin state occurs when the Cl⁻ ligand of [Fe(Papy₂O)(Cl)] (**2**) is replaced with CN⁻. The HS complex **2** is converted into a LS cyanide adduct [Fe(Papy₂O)(CN)] upon addition of one equiv. of (Et₄N)(CN) to a solution of **2** in DMF (EPR data, Figure 5). This change in spin state on going from **2** to [Fe(Papy₂O)(CN)] supports the notion that the spin state of the Fe^{III} center is controlled by the Fe^{III}-N_{amido} and Fe^{III}-O_{phen} interactions which

Figure 3. Thermal ellipsoid plot of **2** (at the 50% probability level)Figure 4. Thermal ellipsoid plot of **3** (at the 50% probability level)

compete against each other. The competing effect of these two interactions appears to be similar enough so that addition of a strong sixth ligand like CN^- results in a switch in the spin state during the $[\text{Fe}(\text{Papy}_2\text{O})(\text{Cl})] \rightarrow [\text{Fe}(\text{Papy}_2\text{O})(\text{CN})]$ transformation.

At this point it is also important to note that the LS species $[\text{Fe}(\text{Papy}_2\text{O})(\text{CN})]$ is quite unstable and can only be studied by low temperature spectroscopy. All attempts to isolate this complex as a solid product have failed so far. In contrast, the analogous CN^- adduct $[\text{Fe}(\text{Papy}_3)(\text{CN})]^+$ (a similar complex with *no* $\text{Fe}^{\text{III}}-\text{O}_{\text{phen}}$ bond) is LS and very stable.^[6] Clearly, the change in spin state converts a stable complex **2** into an unstable species $[\text{Fe}(\text{Papy}_2\text{O})(\text{CN})]$. Since HS complexes with $\text{Fe}^{\text{III}}-\text{O}_{\text{phen}}$ bonds are usually very stable, it is quite evident that forcing the HS complex **2** (with $\text{Fe}^{\text{III}}-\text{O}_{\text{phen}}$ bond) into a LS ($t_{2g}^5 e_g^0$) configuration in $[\text{Fe}(\text{Papy}_2\text{O})(\text{CN})]$ reduces its stability, presumably by minimizing the $d_{\pi}-p_{\pi}$ bonding interaction. Reduction of the $\text{M}^{\text{III}}-\text{O}_{\text{phen}}$ bonding interaction has been noted for Co^{III}

Table 1. Selected bond lengths [\AA] and angles [$^\circ$] for complexes **1**, **2** and **3**

| Complex 1 | | | |
|--------------|------------|---------------|------------|
| Fe–N(1) | 2.069(4) | Fe–N(4) | 2.164(5) |
| Fe–N(2) | 2.192(5) | Fe–O(1) | 1.964(4) |
| Fe–N(3) | 2.059(4) | Fe–O(3) | 1.959(4) |
| C(19)–N(3) | 1.311(7) | C(19)–O(4) | 1.243(7) |
| C(7)–N(1) | 1.307(7) | C(7)–O(2) | 1.229(7) |
| O(3)–Fe–O(1) | 92.91(16) | O(3)–Fe–N(3) | 79.79(17) |
| O(1)–Fe–N(3) | 113.73(17) | O(3)–Fe–N(1) | 107.98(18) |
| O(1)–Fe–N(1) | 80.15(17) | N(3)–Fe–N(1) | 164.22(19) |
| O(3)–Fe–N(4) | 155.35(18) | O(1)–Fe–N(4) | 92.40(18) |
| N(3)–Fe–N(4) | 76.04(19) | N(1)–Fe–N(4) | 96.6(2) |
| O(3)–Fe–N(2) | 94.06(18) | O(1)–Fe–N(2) | 154.92(17) |
| N(3)–Fe–N(2) | 91.23(18) | N(1)–Fe–N(2) | 74.77(18) |
| N(4)–Fe–N(2) | 91.23(19) | | |
| Complex 2 | | | |
| Fe–N(1) | 2.1449(12) | Fe–N(4) | 2.1489(12) |
| Fe–N(2) | 2.2065(11) | Fe–O(2) | 1.8745(9) |
| Fe–N(3) | 2.0172(12) | Fe–Cl | 2.3822(4) |
| C(9)–N(3) | 1.3472(17) | C(9)–O(1) | 1.2532(17) |
| O(2)–Fe–N(3) | 91.08(4) | N(1)–Fe–N(2) | 77.61(4) |
| O(2)–Fe–N(1) | 104.91(4) | N(4)–Fe–N(2) | 75.33(4) |
| N(3)–Fe–N(1) | 85.98(5) | O(2)–Fe–Cl | 95.99(3) |
| O(2)–Fe–N(4) | 102.47(4) | N(3)–Fe–Cl | 171.52(4) |
| N(3)–Fe–N(4) | 94.65(5) | N(1)–Fe–Cl | 87.68(3) |
| N(1)–Fe–N(4) | 152.60(5) | N(4)–Fe–Cl | 88.40(3) |
| O(2)–Fe–N(2) | 172.92(4) | N(2)–Fe–Cl | 90.70(3) |
| N(3)–Fe–N(2) | 82.45(4) | | |
| Complex 3 | | | |
| Fe–N(1) | 2.0142(14) | Fe–N(4) | 2.1553(15) |
| Fe–N(2) | 2.2171(14) | Fe–N(5) | 2.0478(16) |
| Fe–N(3) | 2.1551(15) | Fe–O(1) | 1.8816(12) |
| O(1)–Fe–N(1) | 90.29(6) | N(3)–Fe–N(4) | 152.41(6) |
| O(1)–Fe–N(5) | 96.87(6) | O(1)–Fe–N(2) | 170.35(5) |
| N(1)–Fe–N(5) | 171.20(6) | N(1)–Fe–N(2) | 81.01(5) |
| O(1)–Fe–N(3) | 106.93(6) | N(5)–Fe–N(2) | 92.18(6) |
| N(1)–Fe–N(3) | 86.78(6) | N(3)–Fe–N(2) | 76.93(5) |
| N(5)–Fe–N(3) | 86.23(6) | N(4)–Fe–N(2) | 76.01(5) |
| O(1)–Fe–N(4) | 100.64(6) | N(5)–Fe–N(4) | 89.49(6) |
| N(1)–Fe–N(4) | 94.23(6) | Fe–N(5)–C(22) | 169.33(15) |

complexes with phenolate ligands in which the t_{2g}^6 configuration of the Co^{III} center eliminates any $d_{\pi}-p_{\pi}$ bonding.^[9] Our work thus far indicates that LS complexes with $\text{Fe}^{\text{III}}-\text{N}_{\text{amido}}$ and $\text{Fe}^{\text{III}}-\text{O}_{\text{phen}}$ bonds are inherently unstable. We must comment here that our conclusion regarding weakening of the $\text{Fe}^{\text{III}}-\text{O}_{\text{phen}}$ interaction in LS complexes is preliminary and the final word on the stability of LS versus HS Fe^{III} complexes with both $\text{Fe}^{\text{III}}-\text{N}_{\text{amido}}$ and $\text{Fe}^{\text{III}}-\text{O}_{\text{phen}}$ coordination will require more in-depth studies. Such studies are in progress in this laboratory at the present time.

Finally, we like to point out that complexes **2** and **3** are quite stable toward hydrolysis and do not give rise to species with a $(\mu\text{-oxo})\text{diiron(III)}$ core. For some time now we have maintained that the presence of an $\text{Fe}^{\text{III}}-\text{N}_{\text{amido}}$ bond stabilizes the Fe^{III} center to a great extent and prevents both

Table 2. Comparison of Fe^{III}–N_{amido} and Fe^{III}–O_{phen} (or S_{thio}) bond lengths, with spin state (on Fe^{III}) and half wave reduction potential (vs. SCE) for six coordinate Fe^{III} complexes

| Complex | No. of Fe ^{III} –N _{amido} bonds | Fe ^{III} –N _{amido} (Å) ^[a] | Fe ^{III} –O _{phen} (or S _{thio}) ^[a] (Å) | Spin state of Fe ^{III} | E _{1/2} (V) (DMF) | Reference |
|--|--|--|---|---------------------------------|----------------------------|-----------|
| [Fe(Papy ₃)(Cl)] ⁺ | 1 | 1.8559(17) | | LS | –0.03 | 6 |
| [Fe(Papy ₃)(CN)] ⁺ | 1 | 1.858(2) | | LS | –0.01 | 6 |
| [Fe(Papy ₂ O)(Cl)] (2) | 1 | 2.0172(12) | 1.8745(9) | HS | –0.51 | this work |
| [Fe(Papy ₂ O)(NCS)] (3) | 1 | 2.0142(14) | 1.8816(12) | HS | | this work |
| [Fe(Prpep) ₂] ⁺ | 2 | 1.955(2) | | LS | –0.10 | 12 |
| [Fe(Pyep) ₂] ⁺ | 2 | 1.957(4) | | LS | –0.31 | 11 |
| [Fe(PyepS) ₂] [–] | 2 | 1.954(2) | 2.2291(11) | LS | –1.12 | 14 |
| [Fe(PyepO) ₂] [–] (1) | 2 | 2.064(4) | 1.962(4) | HS | –1.08 | this work |
| [Fe(Py ₃ P) ₂] [–] | 4 | 1.962(2) | | LS | –0.95 | 13 |
| [Fe(MePy ₃ P) ₂] [–] | 4 | 1.955(3) | | LS | –1.05 | 13 |

^[a] Average bond length when more than one bond is present.

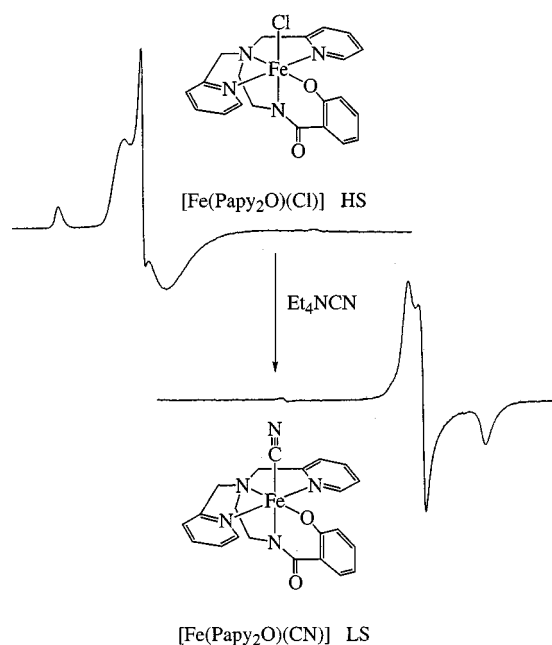


Figure 5. Conversion of HS [Fe(Papy₂O)(Cl)] (2) to LS [Fe(Papy₂O)(CN)] upon addition of (Et₄N)(CN); EPR settings: DMF/MeOH (10:1) glass, T = 80 K, microwave power 13 mW, microwave frequency 9.43 GHz, modulation frequency 100 KHz, modulation amplitude 2 G; the g values for 2 are 9.05, 4.22 and 4.17, and for [Fe(Papy₂O)(CN)] g = 2.39, 2.27 and 1.87

hydrolytic decomposition and formation of oxo- or hydroxo-bridged iron species which are often the thermodynamic end products in iron chemistry.^[10,13] Since the complexes with the Papy₂O^{2–} ligand contain only one Fe^{III}–N_{amido} bond, we have attempted to synthesize directly the corresponding (μ-oxo)diiron(III) complex. However, addition of 2 equiv. of Papy₂O^{2–} to (Et₄N)₂[Fe₂OCl₆] [a pre-formed (μ-oxo)diiron(III) synthon] resulted in the isolation of complex 2 rather than the expected μ-oxo species [(μ-oxo)diiron(III)]₂O. This further supports our previous remarks that complexes with Fe^{III}–N_{amido} bonds do not form oxo-bridged dimers (or polymers), which translates into an enhanced stability of these complexes towards hydrolytic decomposition.

Conclusion

In conclusion, we have prepared and structurally characterized three stable complexes that contain both Fe^{III}–N_{amido} and Fe^{III}–O_{phen} bonds. In previous studies, it has been shown that carboxamido nitrogens (N_{amido}) are strong donors and their coordination to iron usually results in LS Fe^{III} complexes. Previous studies have also shown that complexes with O_{phen} comprise HS Fe^{III} centers. The complexes reported herein now indicate that these two donor atoms in the same molecule influence the spin state of the Fe^{III} center in the opposite sense. Overall, the resulting complexes are HS and so far, no LS complex with both Fe^{III}–N_{amido} and Fe^{III}–O_{phen} bonds has been isolated. It thus appears that the effect of the phenolato oxygen to afford HS Fe^{III} species overrides the spin-pairing trend of the carboxamido nitrogen in Fe^{III} complexes. In the case of Fe^{III} complexes of the Papy₂O^{2–} ligand (which has one N_{amido} and one O_{phen} donor), the overriding effect of O_{phen} can just be compensated by adding a strong sixth ligand (like CN[–]). The resulting LS complex [Fe(Papy₂O)(CN)] is, however, unstable. Since similar LS Fe^{III} complexes with no Fe^{III}–O_{phen} bond(s) are stable entities, it now appears that Fe^{III}–O_{phen} bonds impart instability to LS Fe^{III} complexes.

Experimental Section

Physical Measurements: A Perkin–Elmer 1600 FTIR spectrophotometer was used to monitor the IR spectra. ¹H NMR spectra were recorded on a Bruker 250 MHz spectrometer. EPR spectra were monitored at X-band frequencies on a Bruker ESP-300 spectrometer. Electrochemical measurements were performed with standard Princeton Applied Research instrumentation and a Pt inlay electrode. Potentials were measured at 25 °C versus an aqueous saturated calomel electrode (SCE) as reference.

Materials and Methods: All manipulations were carried out in air. (2-Aminoethyl)bis(2-pyridylmethyl)amine was prepared following a published procedure.^[20] 2-Aminophenol, 2-picolinic acid, 2-acetylsalicylic acid, thionyl chloride (SOCl₂), oxalyl chloride, sodium hydroxide (NaOH), sodium hydride (NaH), and sodium thiocyanate (NaSCN) were purchased from Aldrich Chemical Company

and used without further purification. $(\text{Et}_4\text{N})[\text{FeCl}_4]^{[21]}$ and $[\text{Fe}(\text{DMF})_6](\text{ClO}_4)_3^{[22]}$ were prepared by following published procedures. *N,N'*-dimethylformamide (DMF) was distilled from BaO while tetrahydrofuran (THF) and toluene were distilled from Na/benzophenone prior to use. Dichloromethane (CH_2Cl_2) and acetonitrile (CH_3CN) were distilled from CaH_2 prior to use.

Preparation of PypepOH₂: 2-picolinic acid (5.00 g, 41 mmol) was dissolved in neat SOCl_2 (10–20 mL) and warmed to 50 °C until a clear deep purple solution remained (approx. 1 h). The excess SOCl_2 was removed under vacuum and the purple residue was triturated twice with THF to remove traces of HCl. The purple solid was then redissolved in THF (30 mL) and added to a solution of 2-aminophenol (4.40 g, 41 mmol) and Et_3N (6.30 g, 62 mmol) in THF (50 mL) at 0 °C. The mixture was then heated to reflux for 5 h. Following a brief cooling period, triethylamine hydrochloride was filtered off, and the volatiles were removed by rotary evaporation. The remaining residue was triturated twice with THF and recrystallized from $\text{MeOH}/\text{H}_2\text{O}$ (1:10 v/v) (6.90 g, 78% yield). ^1H NMR (250 MHz, CDCl_3): δ = 6.85 (t, 1 H, ArH), 7.00 (d, 1 H, ArH), 7.08 (t, 2 H, ArH), 7.47 (t, 1 H, ArH), 7.87 (t, 1 H, ArH), 8.23 (d, 1 H, ArH), 8.58 (d, 1 H, ArH), 10.16 (s, 1 H, NH). Selected FTIR absorption bands (KBr pellet): $\tilde{\nu}$ = 3308 (m, N–H), 3072 (m, O–H), 1653 (s, C=O), 1593 (s), 1543 (s), 1458 (s), 1434 (m), 1370 (m), 1284 (m), 1230 (m), 1098 (w), 1038 (w), 932 (w), 852 (w), 757 (s), 738 (s), 691 (s), 618 (w), 594 (w) cm^{-1} .

NaPapy₂OH: 2-Acetylsalicylic acid (1.40 g, 7.5 mmol) was dissolved in neat oxalyl chloride (10–20 mL) and warmed to 40 °C until a clear solution remained (approx. 1 h). Excess oxalyl chloride was removed under vacuum and the clear oil was triturated twice with THF to remove traces of HCl. The residue was then redissolved in THF (10 mL) and added dropwise to a solution of (2-aminoethyl)bis(2-pyridylmethyl)amine (1.80 g, 7.5 mmol) and triethylamine (0.90 g, 9.0 mmol) in THF (25 mL) at 0 °C. The mixture was warmed to room temperature and allowed to stir for 12 h, at which point 6 M NaOH (20 mL) was added. Volatiles were removed by rotary evaporation, the residue was made neutral with 12 M HCl, and extracted with CH_2Cl_2 (3×20 mL). The combined extracts

were dried over MgSO_4 and volatiles were removed under vacuum to yield a gummy yellow residue (crude Papy_2OH_2 : 2.30 g, 6.2 mmol). Sodium metal (0.14 g, 6.2 mmol) was dissolved in methanol (10 mL) and added to the residue. The solution was stirred for 1 h and then the solvent was removed under vacuum. The remaining yellow solid, NaPapy_2OH , was used without further purification (2.40 g, 83% yield). ^1H NMR (250 MHz, $[\text{D}_6]\text{DMSO}$): δ = 2.56 (t, 2 H, CH_2), 3.40 (m, 2 H, CH_2), 3.78 (s, 4 H, CH_2), 6.08 (t, 1 H, ArH), 6.36 (d, 1 H, ArH), 6.87 (t, 1 H, ArH), 7.19 (t, 2 H, ArH), 7.63 (m, 5 H, ArH), 8.44 (d, 2 H, ArH). Selected FTIR absorption bands (KBr pellet): $\tilde{\nu}$ = 3051 (w), 2933 (w), 1625 (s), 1594 (s), 1466 (s), 1438 (s), 1390 (m), 1342 (m), 1256 (m), 1150 (m), 860 (w), 758 (s), 704 (m), 567 (w), 543 (w) cm^{-1} .

Na[Fe(PypepO)₂] (1): PypepOH₂ (0.24 g, 1.1 mmol) was dissolved in DMF (25 mL) and to this was added solid NaH (0.05 g, 2.2 mmol). The mixture was stirred for 2 h and then a batch of $[\text{Fe}(\text{DMF})_6](\text{ClO}_4)_3$ (0.43 g, 0.55 mmol) dissolved in DMF (5 mL) was added to it. The resultant deep green solution was allowed to stir for 2 h at 25 °C. Next, the solvent was removed under vacuum and the residue was dissolved in CH_3CN (10 mL). The solution was then stored at –20 °C for 3 days. The dark green microcrystalline solid thus obtained was collected by filtration (0.27 g, 42% yield). $\text{C}_{29}\text{H}_{23.5}\text{FeN}_{6.5}\text{NaO}_4$ (605.58 for $\text{Na}[\text{Fe}(\text{PypepO})_2] \cdot 2.5 \text{CH}_3\text{CN}$): calcd. C 57.47, H 3.91, N 15.03; found C 57.21, H 3.85, N 15.21. Selected FTIR absorption bands (KBr pellet): $\tilde{\nu}$ = 1670 (s), 1614 (s), 1593 (s, C=O), 1567 (s), 1464 (s), 1388 (m), 1274 (s), 1248 (m), 1098 (m), 1020 (w), 937 (w), 863 (w), 803 (w), 754 (m), 742 (m), 692 (w), 642 (w), 611 (w), 575 (w), 562 (w), 501 (w) cm^{-1} .

[Fe(Papy₂O)(Cl)] (2): A portion of solid NaH (0.01 g, 0.43 mmol) was added to NaPapy_2OH (0.16 g, 0.43 mmol) dissolved in DMF (10 mL) and the mixture was stirred for 2 h. To this solution was added a solution of $(\text{Et}_4\text{N})[\text{FeCl}_4]$ (0.14 g, 0.43 mmol) dissolved in DMF (5 mL) and the resultant deep red solution was allowed to stir for an additional 1 h. The DMF solvent was then removed under vacuum and the residue was dissolved in CH_3CN (20 mL). The red solution was stored at –20 °C overnight. The resultant deep red microcrystalline solid was then filtered off and dried under

Table 3. Crystallographic data for $\text{Na}[\text{Fe}(\text{PypepO})_2] \cdot 2.5\text{CH}_3\text{CN}$ (**1**·2.5 CH_3CN), $[\text{Fe}(\text{PapyO})(\text{Cl})] \cdot 2\text{CH}_3\text{CN}$ (**2**·2 CH_3CN), and $[\text{Fe}(\text{PapyO})(\text{NCS})] \cdot \text{toluene}$ (**3**·toluene)

| | 1 ·2.5 CH_3CN | 2 ·2 CH_3CN | 3 ·toluene |
|---|--|--|--|
| Empirical formula | $\text{C}_{29}\text{H}_{23.5}\text{FeN}_{6.5}\text{NaO}_4$ | $\text{C}_{25}\text{H}_{26}\text{ClFeN}_6\text{O}_2$ | $\text{C}_{29}\text{H}_{28}\text{FeN}_5\text{O}_2\text{S}$ |
| Molecular weight | 605.88 | 533.82 | 566.47 |
| <i>a</i> [Å] | 10.7660(10) | 15.3649(7) | 9.4884(4) |
| <i>b</i> [Å] | 13.0305(12) | 11.3058(5) | 22.1746(10) |
| <i>c</i> [Å] | 20.5973(19) | 15.8124(8) | 12.9277(6) |
| β [°] | 95.239(2) | 115.7740(10) | 94.1370(10) |
| <i>V</i> [Å ³] | 2877.4(5) | 2473.5(2) | 2712.9(2) |
| <i>Z</i> | 4 | 4 | 4 |
| Crystal system | monoclinic | monoclinic | monoclinic |
| Space group | $P2_1/n$ | $P2_1/c$ | $P2_1/n$ |
| ρ [g·cm ^{–3}] | 1.399 | 1.433 | 1.387 |
| <i>T</i> [K] | 90(2) | 90(2) | 90(2) |
| abs coeff, μ , mm ^{–1} | 0.585 | 0.753 | 0.669 |
| GOF ^[a] on <i>F</i> ² | 0.961 | 0.960 | 1.019 |
| <i>R</i> _{<i>i</i>} ^[b] | 6.23 | 3.26 | 4.12 |
| <i>R</i> _w ^[c] | 15.26 | 7.77 | 9.13 |

^[a] GOF = $[\sum[w(F_o^2 - F_c^2)^2]/\sum[w(F_o^2)]]^{1/2}$ (*M* = number of reflections, *N* = number of parameters refined). ^[b] $R_1 = \sum|F_o - F_c|/\sum|F_o|$. ^[c] $R_w = [\sum[w(F_o^2 - F_c^2)^2]/\sum[w(F_o^2)]]^{1/2}$.

vacuum (0.16 g, 70% yield). C₂₅H₂₆ClFeN₆O₂ (533.55 for [Fe(Papy₂O)(Cl)]·2CH₃CN): calcd. C 56.23, H 4.91, N 15.75; found C 56.19, H 4.96, N 15.28. Selected FTIR absorption bands (KBr pellet): $\tilde{\nu}$ = 1597 (m, C=O), 1571 (s), 1533 (s), 1444 (s), 1360 (s), 1290 (w), 1244 (w), 1102 (w), 1024 (w), 895 (w), 768 (s), 704 (w), 658 (w) cm⁻¹.

[Fe(Papy₂O)(NCS)] (3): To a solution of NaPapy₂OH (0.21 g, 0.55 mmol) in DMF (10 mL) was added a batch of solid NaH (0.013 g, 0.55 mmol) and the mixture was allowed to stir for 2 h. To this solution was then added a batch of [Fe(DMF)₆](ClO₄)₃ (0.43 g, 0.55 mmol) dissolved in DMF (5 mL) and the purple/red solution was stirred for an additional 1 h. At this point, a solution of NaSCN (0.067 g, 0.83 mmol) in DMF (1 mL) was added and the color of the solution changed to red/brown. The DMF solvent was removed under vacuum and the residue was dissolved in THF (30 mL). The solution was stored at -20 °C overnight. The deep red needles were collected by filtration (0.15 g, 50% yield). C₂₆H₂₈FeN₅O₃S (546.17 for [Fe(Papy₂O)(NCS)]·THF): calcd. C 57.13, H 5.17, N 12.82; found C 57.27, H 5.19, N 12.74. Selected FTIR absorption bands (KBr pellet): $\tilde{\nu}$ = 2046 (s, SCN), 1594 (m, C=O), 1570 (m), 1534 (m), 1445 (m), 1352 (m), 1103 (w), 1024 (w), 763 (m,) cm⁻¹.

Crystal Structure Analysis: Deep black/green crystals of Na[Fe(Py₂pepO)₂]·2.5CH₃CN (**1**·2.5CH₃CN) and dark red crystals of [Fe(Papy₂O)(Cl)]·2CH₃CN (**2**·2CH₃CN) were each grown from CH₃CN at -20 °C. Black/red X-ray quality plates of [Fe(Papy₂O)(NCS)]·toluene (**3**·toluene) were grown from toluene/CH₂Cl₂ (3:1). Diffraction data for all complexes were collected at 90 K on Bruker SMART 1000 diffractometer. Mo-K α (0.71073 Å) radiation was used in all cases and the data were corrected for absorption. The structures were solved using the standard SHELXS-97 package. Machine parameters, crystal data, and data collection parameters for **1**·2.5CH₃CN, **2**·2CH₃CN, and **3**·toluene are summarized in Table 3, while selected bond lengths and angles are listed in Table 1.

CCDC-166560, -166561 and -166552 contain the supplementary crystallographic data for complexes **1**·2.5CH₃CN, **2**·2CH₃CN, and **3**·toluene, respectively. These data can be obtained free of charge at www.ccdc.cam.ac.uk/conts/retrieving.html [or from the Cambridge Crystallographic Data Centre, 12, Union Road, Cambridge CB2 1EZ, UK; Fax: (internat.) +44-1223/336-033; E-mail: deposit@ccdc.cam.ac.uk].

Acknowledgments

Financial support from NSF (CHE-9818492) and NIH (GM 61636) is gratefully acknowledged. The Bruker SMART 1000 diffractometer was funded in part by an NSF Instrumentation Grant CHE-9808259.

- [1] E. I. Solomon, T. C. Brunold, M. I. Davis, J. N. Kemsley, S. -K. Lee, N. Lehnert, F. Neese, A. J. Skulan, Y. -S. Yang, J. Zhou, *Chem. Rev.* **2000**, *100*, 235–350.
- [2] *Biomimetic Oxidations Catalyzed by Transition Metal Complexes* (Ed.: B. Meunier), Imperial College Press, London, **1999**.
- [3] D. S. Marlin, P. K. Mascharak, in *Encyclopedia of Catalysis: Biomimetic Catalysis by Models of Non-Heme Iron Enzymes* (Ed.: I. T. Horváth), John Wiley & Sons, Inc. New York, in press.
- [4] T. J. Collins, S. W. Gordon-Wylie, M. J. Bartos, C. P. Horwitz, C. G. Woome, S. A. Williams, R. E. Patterson, L. D. Vuocolo, S. A. Paterno, S. A. Strazisar, D. K. Peraino, C. A. Dudash, in *Green Chemistry: Frontiers in Benign Chemical Syntheses and Processes* (Eds.: P. T. Anastas and T. C. Williamson), Oxford University Press, Oxford, **1998**, 46.
- [5] D. S. Marlin, P. K. Mascharak, *Chem. Soc. Rev.* **2000**, *29*, 69–74.
- [6] J. M. Rowland, M. M. Olmstead, P. K. Mascharak, *Inorg. Chem.* **2001**, *40*, 2810–2817.
- [7] C. Stockheim, L. Hoster, T. Weyhermüller, K. Wiegardt, B. Nuber, *J. Chem. Soc., Dalton Trans.* **1996**, 4409–4416.
- [8] U. Auerbach, U. Eckert, K. Wiegardt, B. Nuber, J. Weiss, *Inorg. Chem.* **1990**, *29*, 938–944.
- [9] U. Auerbach, T. Weyhermüller, K. Wiegardt, B. Nuber, E. Bill, C. Butzlaff, A. X. Trautwein, *Inorg. Chem.* **1993**, *32*, 508–519.
- [10] D. S. Marlin, M. M. Olmstead, P. K. Mascharak, *Inorg. Chim. Acta* **2000**, *297*, 106–114.
- [11] X. Tao, D. W. Stephan, P. K. Mascharak, *Inorg. Chem.* **1987**, *26*, 754–759.
- [12] S. J. Brown, M. M. Olmstead, P. K. Mascharak, *Inorg. Chem.* **1990**, *29*, 3229–3234.
- [13] D. S. Marlin, M. M. Olmstead, P. K. Mascharak, *Inorg. Chem.* **1999**, *38*, 3258–3260.
- [14] J. C. Noveron, M. M. Olmstead, P. K. Mascharak, *Inorg. Chem.* **1998**, *37*, 1138–1139.
- [15] S. Kimura, E. Bill, E. Bothe, T. Weyhermüller, K. Wiegardt, *J. Am. Chem. Soc.* **2001**, *123*, 6025–6039.
- [16] S. Wang, L. Wang, X. Wang, Q. Luo, *Inorg. Chim. Acta* **1997**, *254*, 71–77.
- [17] K. Ramesh, R. Mukherjee, *J. Chem. Soc., Dalton Trans.* **1992**, 83–89.
- [18] J. W. Hwang, K. Govindaswamy, S. A. Koch, *Chem. Commun.* **1998**, 1667–1669.
- [19] S. A. Koch, M. Millar, *J. Am. Chem. Soc.* **1982**, *104*, 5255–5257.
- [20] G. S. Matouzenko, A. Bousseksou, S. Lecocq, P. J. Van Koningsbruggen, M. Perrin, O. Kahn, A. Collet, *Inorg. Chem.* **1997**, *36*, 2975–2981.
- [21] A. P. Ginsberg, M. B. Robin, *Inorg. Chem.* **1963**, *2*, 817–822.
- [22] J. Hodgkinson, R. B. Jordan, *J. Am. Chem. Soc.* **1973**, *95*, 763–768.

Received July 18, 2001
[I01267]